Available online at www.sciencedirect.com

ScienceDirect

Journal of Molecular Liquids 00 (2024) 1–17

JML

Canonical partition function and distance dependent correlation functions of a quasi-one-dimensional system of hard disks

V.M. Pergamenshchik*[a,b], T. Bryk[c,d], A. Trokhymchuk[c]

[a]Institute of Physics, National Academy of Sciences of Ukraine, prospekt Nauky, 46, Kyiv 03039, Ukraine, *victorpergam@yahoo.com
[b]Center for Theoretical Physics, Polish Academy of Sciences, Al. Lotników 32/46, 02-668, Warsaw, Poland
[c]Institute for Condensed Matter Physics, NAS of Ukraine, 1 Svientsistsky Str, Lviv, 79011, Ukraine
[d]Institute of Applied Mathematics and Fundamental Sciences,
Lviv National Polytechnic University, UA-79013 Lviv, Ukraine

Abstract

The canonical NLT partition function of a quasi-one dimensional (q1D) one-file system of equal hard disks [J. Chem Phys. **153**, 144111 (2020)] provides an analytical description of the thermodynamics and ordering in this system (a pore) as a function of linear density Nd/L where d is the disk diameter. We derive the analytical formulae for the distance dependence of the translational pair distribution function and the distribution function of distances between next neighbor disks, and then demonstrate their use by calculating the translational order in the pore. In all cases, the order is found to be of a short range and to exponentially decay with the disks' separation. The correlation length presented for different pore widths and densities shows a non-monotonic dependence with a maximum at $Nd/L = 1$ and tends to the 1D value for a vanishing pore width. The results indicate a special role of this density when the pore length L is equal exactly to N disk diameters. Comparison between the theoretical results for an infinite system and the results of a molecular dynamics simulation for a finite system with periodic boundary conditions is presented and discussed.

Keywords: quasi-one-dimensional pore, hard-disk system, partition function, correlation functions
PACS: 64.75.Yz, 61.20.Gy, 61.20.Ja, 61.20.Ne, 05.10.-a

1. Introduction

The statistical description of many-particle systems must deal with many, even infinite number of degrees of freedom and as many integrals. As this limit can be studied only theoretically, the analytical results and particularly exact ones are of great importance. To solve a statistical mechanical problem implies to reduce the problem of calculation of its partition function (PF) and pair correlation functions to a finite number of dimensions, finite number of integrals and other mathematical actions. This is most often a task impossible and we try to learn the physics of many-body system and develop the appropriate mathematical tools by studying simplified models. In particular, a strong simplification can be achieved by considering geometries with reduced dimensionality and, in particular, one-dimensional (1D). A great number of 1D models considered in the last century and summarized in the book [1] has proved to be very usefully related to the physics in two and three dimensions. In the theory of liquids, modeling molecules as hard spheres, the distinguished example of the 1D physics is the exact solution for the PF of a 1D gas of hard core molecules, now known as Tonks' gas [2].

The 1D Tonks gas is much simpler than any 2D system, nevertheless Tonks' solution has become the analytical platform for further expansion into the world of 2D hard disk (HD) systems via moving to certain quasi-one-dimensional (q1D) models. The simplest q1D HD system is such that each disk can touch no more than one next neighbor from both sides (the so-called single-file system); the width of such q1D pore must be below $(\sqrt{3}/2+1)d$ where d is the HD diameter. The analytical theory of HDs in q1D pore was first considered by Wojciechowski et al [3] for a system periodically replicated in the transverse direction. Later Kofke and Post [4] proposed an approach that enables one to consider HDs in a q1D pore in the thermodynamic limit using the well-known transfer matrix method introduced in statistical physics by Kramers and Wannier [5]. This theory has become the main tool in studying a q1D single-file HD system [6, 7, 8, 9, 10, 11] that allowed one to address also q1D systems of non-circular particles (e.g., [12]). The virial expansion for disks in the q1D geometry has been addressed by Mon [13]. Thanks to the analytical methods nowadays HDs in the q1D geometry have been intensively used for calculations of thermodynamic as a model glass former to study glass transitions and HDs' dynamics [9, 14, 15, 16]. The approximate analytical theory for HDs was also developed for one- and two-dimensional random pore geometry by the scaled particle method [17]. The new interest has been brought about by the studies of actual physical ultracold systems such as Bose-Einstein condensates created in practically 1D or q1D electromagnetic traps [18]. Although mathematically quantum and classical gases are very different, the classical 1D and q1D models can provide some technical and even physical insight.

The transfer matrix method is essentially related to the pressure-based NPT ensemble which does not directly predict pressure as a function of system's width D and length L as the Gibbs free energy is parameterized by the pressure P. Another peculiarity is that the transfer matrix approach essentially employs the periodic boundary conditions along the pore which allows one to reduce the PF to the trace of the transfer matrix [4]. Recently one of us derived analytically the canonical NLT PF of a q1D HD single-file system (from now on q1D implies also single-file system) both for a finite number of disks N and in the thermodynamic limit [19]. Although the derivation of the PF in [19] has used certain approximation which is addressed in more detail in the next section, the obtained results provide convenient analytical tools. In particular, the PF of a NLT ensemble is not related to the periodic boundary conditions and finding the thermodynamic properties of a q1D HD system for given L and D is reduced to solving single transcendental equation which can be easily done numerically. The PF, pressure along and across the pore, distribution of the contact distances between neighboring HDs along the pore, and distribution of HD centers across the pore for given linear density $\rho = Nd/L$ are found analytically. In this paper we derive and employ another fundamental thermodynamic quantity, the pair distribution function (PDF).

The transfer matrix method directly gives the leading correlation length that describes the correlations between the disks' transverse coordinates y_i and y_{i+n} as a function of the difference n between their order numbers [6, 7, 8, 9, 10, 11]. At the same time, the most important longitudinal ordering is related to PDFs that are functions of the actual distance R between disks along the system. The analytical formula for such PDF $g_{1D}(R)$ is known only for a 1D gas of noninteracting (Tonks' gas) [22, 20, 21] and interacting [21] hard core molecules . In a q1D system, finding the PDF $g(R)$ for large R by the transfer matrix method directly from its definition is admittedly a formidable problem [7]. The large R behavior of the PDF is possible to get by means of the following nontrivial numerical procedures: either by inverse Fourier transform of the structure factor obtained from the joint solution of two integral equations [9], or by first planting the system's configuration from the transfer matrix eigenstates and then averaging over these planted configurations [11]. The main goal of this paper is to develop an alternative, analytical approach to the PDFs of a q1D HD system based on the NLT ensemble PF, which is not related to periodic boundary conditions along the pore, and demonstrate its implementation.

From the analytical canonical PF of a q1D HD system [19], we derive a formula for the translational PDF $g(R)$ which requires computing a few integrals and can be straightforwardly implemented numerically. We also derive the PDF for the distance between next neighbors. Both PDFs are presented for an infinite system, but the canonical PF allows one to obtain the formulae for finite systems, too. Usually, the PDF for a 1D gas is derived by resorting to Laplace's transform related to the NPT ensemble [20, 21], but in earlier works Frenkel [22] and Nagamija [23] used a more direct technique related to a converting infinite products into exponentials. We also use the last technique and derive the PDF for a q1D HD system directly from the canonical PF. The method is first demonstrated by application to the PDF of a 1D Tonks gas and the derived formulae then used to calculate the translational PDF $g(R)$ and its correlation length for the range of the q1D pore widths and wide range of linear densities of a q1D HD system. In all cases, the correlations are found to exponentially decay with the disks' separation. The correlation length presented for the total range of the q1D pore widths and different densities shows a non-monotonic density dependence with a maximum at the density $Nd/L = 1$ and, for vanishing pore width, tends to the 1D value of a Tonks gas. The theoretical PDFs $g(R)$ and $g_1(R)$ are compared with the results of molecular dynamic (MD) simulations presented for q1D systems of $N = 400$ and 2000 HDs. It is found that the theoretical and computer simulations results for $g_1(R)$ nearly coincide for high and low densities. At the same time, at the intermediate densities in the vicinity of $\rho \sim 1$, to coincide with the MD results, the theoretical g_1 should be obtained for a slightly higher density. Analysing MD simulations data for PDF $g(R)$, we came to a tentative conclusion that this difference can be attributed to the approximation used in [19] and, possibly, to a pressure difference between a finite system with periodic boundary condition considered in computer simulations and an infinite system considered in the theory.

The paper is structured as follows. The canonical PF and the methods of its calculations are introduced in Sec. 2, and then, in Sec. 3, the formulas for PDFs $g(R)$ and $g_1(R)$ are derived. In Sec. 4, these formulae are used to study the theoretical PDFs, the results are compared with the MD data and discussed in detail. The final Sec.5 is a brief conclusion.

2. The canonical partition function of a q1D HD system

Consider a pore of length L, confined between two parallel hard walls separated by the width D, and filled with N of HDs of diameter $d = 1$. All lengths will be measured in units of HD diameters. The reduced width $\Delta = (D - d)/d$, that gives the actual pore width attainable to HD centers, in the single-file q1D case ranges from 0 in the 1D case to the maximum $\sqrt{3}/2 \approx 0.866$. The i-th disk has two coordinates, x_i along and y_i across the pore; y varies in the range $-\Delta/2 \leq y \leq \Delta/2$; the pore volume is LD. The transverse center-to-center distance between two neighbors, $\delta y_i = y_{i+1} - y_i$, determines the contact distance σ between them along the pore:

$$\begin{aligned} \sigma(\delta y_i) &= \min |x_{i+1}(y_{i+1}) - x_i(y_i)|, \\ \sigma(\delta y_i) &= \sqrt{d^2 - \delta y_i^2}, \\ \sigma_m(\Delta) &= \sqrt{d^2 - \Delta^2} \leq \sigma \leq d\,. \end{aligned} \tag{1}$$

The minimum possible contact distance, σ_m, depends on the pore width Δ and obtains for $\delta y_i = \pm\Delta$ when the two disks are in contact with the opposite walls. Thus, each set of coordinates $\{y\} = y_1, y_2, \ldots, y_N$ determines the correspondent densely packed state of the total length $L'\{y\} = \sum_{i=1}^{N-1} \sigma(\delta y_i)$, which we call condensate [19]. The minimum condensate length (the distance between centers of the first and N th disk) is $(N-1)\sigma_m$, the maximum length can be as large as $(N-1)d$, but it cannot exceed $L-d$, i.e., $(N-1)\sigma_m < L' \leq L'_{\max}$ where $L'_{\max} = \min[(N-1)d, L-d]$.

The PF of this q1D HD system is given by the integral [19]:

$$Z = \Delta \int_{-\infty}^{\infty} \frac{d\alpha}{N!} \int_{(N-1)\sigma_m}^{L'_m} dL' e^{i\alpha L'} (L - 1 - L')^N \left(\int_{\sigma_m}^{1} \frac{d\sigma}{\sqrt{1 - \sigma^2}} \sigma e^{-i\alpha\sigma} \right)^{N-1}, \tag{2}$$

where i is an imaginary unite. To derive the above PF, in [19], the integration over transverse coordinates y was changed to that over $\sigma(\delta y)$. The integration over different δy_i is not independent and so is the integration over $\sigma(\delta y_i)$, but in [19] this integration was performed for each $\sigma(\delta y_i)$ from σ_m to 1 independently. It turns out that the PF obtained under the above approximation coincides with that obtained in [3] for a system periodic in the transverse direction. However, in [19] such periodic condition in y was not imposed. The above approximation is supposed to be valid in the limit of large N as in this limit the main contribution to the PF has to come from the average contact distance $\overline{\sigma}$ which does lie within the range from σ_m to 1. This approximation has allowed one to solve the problem analytically for the system in a box and avoid the periodic boundary condition in x.

It is convenient to rewrite this PF in the exponential form:

$$Z = \frac{\Delta}{N!} \int_{(N-1)\sigma_m}^{L'_m} dL' \int d\alpha e^{S}, \tag{3}$$

where

$$S = i\alpha L' + N \ln(L - 1 - L') + (N - 1) \ln\left(\int_{\sigma_m}^{1} \frac{d\sigma}{\sqrt{1 - \sigma^2}} \sigma e^{-i\alpha\sigma} \right). \tag{4}$$

Equations (3) and (4) give the PF in the general case of a q1D HD system for large N and L.

The integrand of Z is a regular function of α so that the α-integration contour, in particular, its central part that gives the principal contribution to the integral, can be shifted while the ends remain along the real axis. In the thermodynamic limit $N \to \infty$, $L \to \infty$, $Nd/L = \rho = const$, we can compute the PF (3) by the steepest descent method. In the limit $N \to \infty$ the integral (3) is exactly determined by the saddle point which, for given N, L and σ_m, is the stationary point of the function $S(i\alpha, L')$, Eq. (4). It is convenient to introduce real $a = i\alpha$ since α at the saddle point lies on the imaginary axis and the integration contour has to be properly deformed. The two equations $\partial S/\partial a = \partial S/\partial L' = 0$ that determine the saddle point, can be reduced to the single equation for $a = a_N$ which reads:

$$\frac{L}{N} - \frac{1}{a_N} = \frac{I'(a_N)}{I(a_N)}, \tag{5}$$

where

$$I(a_N) = \int_{\sigma_m}^{1} \frac{d\sigma}{\sqrt{1-\sigma^2}} \sigma \exp(-a_N \sigma), \tag{6}$$

$$I'(a_N) = \int_{\sigma_m}^{1} \frac{d\sigma}{\sqrt{1-\sigma^2}} \sigma^2 \exp(-a_N \sigma). \tag{7}$$

The solution a_N of Eq. (5), which gives the total longitudinal pressure $P_L = k_B T a_N / D$ [19] and longitudinal force $k_B T a_N$ [16] where $k_B T$ is Boltzmann's constant times temperature, depends on the per disk pore length L/N and, via σ_m, on the pore width D, and fully determines the free energy. The free energy per disk, F/N, which therefore is the function of the pore length L, pore width D and the temperature T, is $F(L, D, T)/N = -TS(a_N)/N = -Ts_N$ where s_N is system's per disk entropy:

$$s_N = a_N \sigma_N + \ln(L - N\sigma_N) + \frac{N-1}{N} \ln I(a_N), \tag{8}$$

where σ_N is the average value of the contact distance σ in the condensate [i.e., average of $L'/(N-1)$] [19]:

$$\sigma_N = \frac{L}{N} - \frac{1}{a_N}. \tag{9}$$

Finally, for $N \to \infty$, the PF can be cast in the two equivalent forms:

$$\begin{aligned} Z_\infty &= \frac{\varsigma_N \Delta}{N!} \exp(N s_N) \\ &= \frac{\varsigma_N \Delta}{N!} (L - N\sigma_N)^N I(a_N)^{N-1} \exp(N a_N \sigma_N), \end{aligned} \tag{10}$$

where ς_N is the prefacfor $\sim 1/\sqrt{N}$ originated from the Gaussian integration along the steepest descent contour whose exact form is of no need. In the 1D case, all σ's are equal to d and this expression goes over into the Tonks PF Z_{1D} up to the factor Δ^N which in this case represents the independent transverse degrees of freedom: $Z_\infty \to \Delta^N Z_{1D}$ where

$$Z_{1D} = \frac{1}{N!} (L - Nd)^N \theta(L - Nd) \tag{11}$$

and $\theta(x)$ is the step function equal to 1 for $x > 0$ and 0 otherwise. Now consider the general case of a finite system. In what follows, the number of HDs and the total length of a finite system are denoted as n and L_n, respectively (instead of N and L). The integral (2) can be transformed to the one along the real axis α like that:

$$\begin{aligned} Z_{n, L_n} &= \frac{\Delta}{n!} \int_{(n-1)\sigma_m}^{L_m} dL' \, (L_n - 1 - L')^n \\ &\quad \times \int_{-\infty}^{\infty} \frac{d\alpha}{2\pi} \, |I(i\alpha)|^{n-1} \cos\left[L'\alpha + (n-1)\varphi_\alpha\right], \end{aligned} \tag{12}$$

where $L_m = \min(n-1, L_n - 1)$ and

$$\begin{aligned} \varphi_\alpha &= \arg I(i\alpha), \\ I(i\alpha) &= \int_{\sigma_m}^{1} \frac{d\sigma}{\sqrt{1-\sigma^2}} \sigma e^{-i\alpha\sigma} . \end{aligned} \tag{13}$$

Although the Gaussian approximation at the saddle point cannot give an exact result for a system with finite number of disks, choosing the α integration contour passing through the saddle point provides the best convergence of the integrals (which has been confirmed numerically). Hence to compute the PF we shift the central part of the α integration contour downward and integrate over the real variable t along the line $\alpha = -ia_n + t$ that crosses the imaginary axis at $\alpha = -ia_n$. The best choice for the shift a_n is the root of the following modified equation (5):

$$\frac{L_n}{n} - \frac{n-1}{na_n} = \frac{I'(a_n)}{I(a_n)} , \tag{14}$$

whose rhs is defined in Eqs. (6) and (7). Then the PF Z_{n,L_n} can be transformed like that:

$$\begin{aligned} Z_{n,L_n} &= \frac{\Delta}{n!} \int_{(n-1)\sigma_m}^{L_m} dL' e^{a_n L'} \left(L_n - 1 - L'\right)^n \\ &\times \int_{-\infty}^{\infty} \frac{dt}{2\pi} \left(I_s{}^2 + I_c^2\right)^{(n-1)/2} \cos[L't + (n-1)\varphi] . \end{aligned} \tag{15}$$

where

$$\begin{aligned} I_s(t) &= -\int_{\sigma_m}^{1} \frac{d\sigma}{\sqrt{1-\sigma^2}} \sigma e^{-a_n\sigma} \sin(t\sigma) , \\ I_c(t) &= \int_{\sigma_m}^{1} \frac{d\sigma}{\sqrt{1-\sigma^2}} \sigma e^{\,-a_n x} \cos(t\sigma) , \end{aligned} \tag{16}$$

$$\varphi(t) = \arg\left(I_c + iI_s\right) = \begin{cases} \arctan\dfrac{I_s}{I_c} \ , I_c > 0 , \\ \pi + \arctan\dfrac{I_s}{I_c} \ , I_c < 0, I_s > 0 , \\ -\pi + \arctan\dfrac{I_s}{I_c} \ , I_c < 0, I_s < 0 . \end{cases} . \tag{17}$$

The density n/L_n and the reduced pore width Δ, which enter the integrals above via σ_m, fully determine the partition function $Z_{n,\,L_n}$ through Eqs. (14) - (17).

3. Derivation of the PDF from the canonical partition function

The PDF as a function of separation R is the probability to find particle a distance R from another particle whose coordinate x_0 is fixed, say at $x_0 = 0$. Here we derive $g(R)$ for a q1D HD systems directly from the PF Z_N of the canonical NLT ensemble.

The q1D PF $Z_N\{x_i, y_i\}$, Eqs. (3) and (4), is a functional of the particles' longitudinal x coordinates and transverse y coordinates. In the particular case of a q1D system, the general formula for the PDF $g(R)$ equivalent to its definition is obtained from the canonical PF for the N particle system by fixing the x coordinate of n-th disk at $x_n = x$ and then summing over all possible n (the range of n will be clarified later on):

$$g(R) = \frac{1}{\rho} \sum_{n=1} \frac{Z_N\{x_0 = 0, y_0, x_1, y_1, ..., x_n = R, y_n, ..., x_N, y_N\}}{Z_N\{x_0 = 0, y_0, x_1, y_1, ..., x_n, y_n, ...x_N, y_N\}} . \tag{18}$$

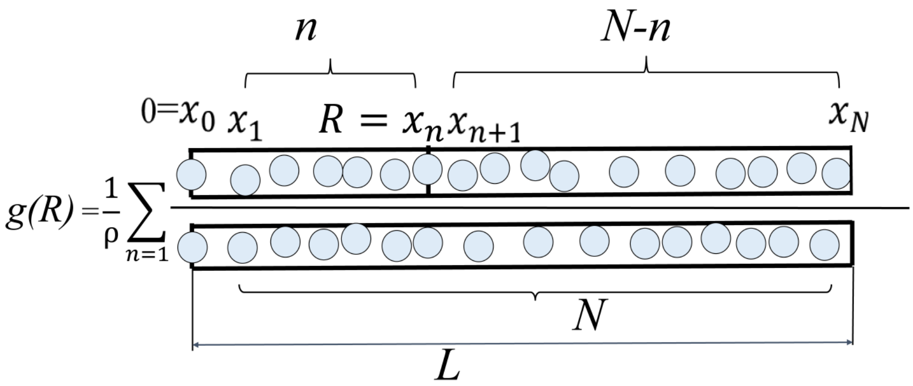

Figure 1. Definition of the pair distribution function $g(R)$ and the three PFs: $Z_{n,R}$ is for $n-1$ free moving disks in the space R in which there are n neighbors of disk 0; $Z_{N-n,L-R}$ is for $N-n$ free disks in the space $L-R$; and Z_N is for N free disks in the space L.

Note that y_0 and y_n are not fixed so that the particles 0 and n can move in the transverse direction. The PF in the nominator splits into a product of two PFs, Z_n for n disks (of which $n-1$ are free to move) in the space $0 < x_k < R$, and $Z_{N-n,L-R}$ for $N-n$ moving disks in the space $R < x_k < L-R-d/2$, Fig. 1:

$$g(R) = \frac{1}{\rho}\sum_{n=1} \frac{Z_{n,R} Z_{N-n,L-R}}{Z_{N,L}}\,. \tag{19}$$

Figure 1 demonstrates that the numbers of free disks, contact distances σ, and the disk-vertical wall contact distance $d/2$ have to be adjusted in each PF individually. As a result, the form of Eq. (5) that determines a_n, is also slightly modified.

Consider first $Z_{n,R}$. We assume that $R > 1$; the case $R < 1$, possible only for $n = 1$, will be considered separately. In the system of size $R > 1$, there are $n-1$ freely moving HDs, $\int dy_0 = \Delta$, n contact distances σ, no vertical walls and thus no contact distances $d/2$. Hence $(R-d-L')^n$ in PF (15) has to be replaced by $(R-L')^{n-1}$ and $I(i\alpha)^{n-1}$ by $I(i\alpha)^n$. Then the PF $Z_{n,R}$ takes the form

$$\begin{aligned} Z_{n,R} \;=\; & \frac{\Delta}{(n-1)!}\int_{n\sigma_m}^{L_{n,m}} dL' e^{a_n L'}\,(R-L')^{n-1} \\ & \times \int_{-\infty}^{\infty} \frac{dt}{2\pi}(I_s{}^2 + I_c{}^2)^{n/2} \cos[L't + n\varphi(t)]\,, \end{aligned} \tag{20}$$

where $L_{n,m} = \min(n, R)$. The angle $\varphi(t)$ is defined in Eq. (17), a_n is the root of equation (14), and the relation between σ_n and a_n is just the properly modified Eq. (9),

$$\sigma_n = \frac{R}{n} - \frac{n-1}{n a_n}\,. \tag{21}$$

Next consider $Z_{N-n,L-R}$ in Eq. (19), the PF for $N-n$ HDs in the range $R < x < L$. Here all disks are free to move, there are $N-n$ contact distances σ, and the single vertical wall at the pore end. Then the PF $Z_{N-n,L-R}$ can be presented in the form

$$Z_{N-n,L-R} \;=\; \frac{1}{(N-n)!}\int_{\sigma_m}^{L_{N-n,m}} dl e^{L' a_{N-n}}(L-R-1/2-L')^{N-n}$$

$$\times \int_{-\infty}^{\infty} \frac{dt}{2\pi} (I_s{}^2 + I_c{}^2)^{(N-n)/2} \cos[L't + (N-n)\varphi(t)] \,, \tag{22}$$

where $L_{N-n,m} = \min(N-n, L-R-1/2)$ and a_{N-n} is the root of the following modified Eq. (5):

$$\frac{L-R-1/2}{N-n} - \frac{1}{a_{N-n}} = \frac{I'(a_{N-n})}{I(a_{N-n})} \,. \tag{23}$$

At last, consider $Z_{N,L}$ in Eq. (19) that is the PF for N HDs in the range $0 < x < L$. Here all disks are free to move, $\int dy_0 = \Delta$, there are N contact distances σ and the single vertical wall at the pore end. Then the PF $Z_{N,L}$ can be presented in the form

$$\begin{aligned} Z_{N,L} &= \frac{\Delta}{N!} \int_{N\sigma_m}^{L_{N,m}} dL' e^{a_N L'} (L - 1/2 - L')^N \\ &\times \int_{-\infty}^{\infty} \frac{dt}{2\pi} (I_s{}^2 + I_c{}^2)^{N/2} \cos[L't + N\varphi(t)] \,, \end{aligned} \tag{24}$$

where $L_{N,m} = \min(N, L-1/2)$ and a_N is the root of the equation (5). Making use of the PFs (20), (22), and (24) in the general formula (19) gives the PDF of a q1D HD system for finite N and L.

The general result for $g(R)$ can be further simplified in the thermodynamic limit. This case, usually considered the most important one, is presented in detail in the next section. To illustrate our method of deriving the PDF directly from the canonical NLT PF we first derive the PDF for 1D Tonks' gas.

3.1. PDF of a q1D HD system in the thermodynamic limit

3.1.1. PDF of an infinitely long 1D HD system (Tonks' gas)

The PDF $g(R)$ for a 1D HD is given by the general formula (19) in which the three PFs are obtained from the Tonks' PF, Eq. (11):

$$g_{1D}(R) = \frac{1}{\rho} \sum_{n=1} \frac{N! |R-n|^{n-1} [L-R-n]^{N-n}}{(n-1)!(N-n)!(L-n)^N} \, \theta(R-n) \,. \tag{25}$$

In the limit $N \to \infty$, neglecting $O(n/N)$, one also has $(N-n)! \cong N!/N^n$ and

$$\begin{aligned} (L-R-n)^{N-n} &= (L-N)^{N-n} \left(1 - \frac{R-n}{N(l_N - 1)}\right)^{N-n} \\ &= (L-N)^{N-n} \left[\exp\left(-\frac{R-n}{l_N-1}\right) + O\left(\frac{n}{N}\right)\right] \\ &\to (L-N)^{N-n} \exp\left(-\frac{R-n}{l_N-1}\right) , \end{aligned} \tag{26}$$

where $l_N = L/N = 1/\rho$. Making use of these results in Eq. (25) and introducing the step function, $\theta(R-n) = 1$ for $R \geq n$ and $\theta(R-n) = 0$ otherwise, one finally obtains

$$g_{1D}(R) = \frac{1}{\rho} \sum_{n=1} \frac{|R-n|^{n-1} \exp\left(-\dfrac{R-n}{l_N-1}\right)}{(n-1)!(l_N-1)^n} \, \theta(R-n) \,, \tag{27}$$

which is the well-known PDF of 1D Tonks' gas [20, 21].

3.1.2. PDF of an infinitely long q1D HD system.

In an infinitely long q1D HD system, the above thermodynamic limit result, Eqs. (3) and (4), is applicable both for $Z_{N,L}$ and $Z_{N-n,L-R}$ as the number of particles $N-n$ and volume $L-R$ are infinite, but the PF $Z_{n,R}$ for the finite n disk system has to be found directly from the general formula (15) [or from the original form (12) without the contour shift]. Adjusting Eqs. (8)-(10) to the above PFs of interest, one has:

$$\begin{aligned} Z_{N-n,L-R} &= \frac{\varsigma_{N-n}}{(N-n)!}[L-R-(N-n)\sigma_{N-n}]^{N-n}\exp[(N-n)\widetilde{s}_{N-n}], \\ Z_{N,L} &= \frac{\varsigma_N\Delta}{N!}(L-N\sigma_N)^N\exp(N\widetilde{s}_N). \end{aligned} \tag{28}$$

Here $\widetilde{s}_{N-n} = a_{N-n}\sigma_{N-n} + \ln I(a_{N-n})$ and $\widetilde{s}_N = a_N\sigma_N + \ln I(a_N)$, where the pair σ_N, a_N is determined by $l_N = L/N = 1/\rho$ from the Eqs. (5) and (9) and the pair σ_{N-n}, a_{N-n} by $l_{N-n} = (L-R)/(N-n)$ from similar equations

$$\begin{aligned} l_{N-n} - \frac{1}{a_{N-n}} &= \frac{I'(a_{N-n})}{I(a_{N-n})}, \\ \sigma_{N-n} &= l_{N-n} - \frac{1}{a_{N-n}}. \end{aligned} \tag{29}$$

Substituting these expressions in the general formula (19) for $g(R)$ and taking into account that in the thermodynamic limit the preexponential factors ς_N and ς_{N-n} are equal, we get:

$$\begin{aligned} g(R) &= \frac{1}{\rho}\sum_{n=1}\frac{Z_{n,R}N![L-R-(N-n)\sigma_{N-n}]^{N-n}}{(N-n)!(L-N\sigma_N)^N} \\ &\quad\times\exp[N(\widetilde{s}_{N-n}-\widetilde{s}_N)-n\widetilde{s}_{N-n}]. \end{aligned} \tag{30}$$

Now we find $\widetilde{s}_{N-n}$ by expanding about $\widetilde{s}_N$ and using the smallness of n/N. First, up to $O(n/R)$, one has $N(\widetilde{s}_{N-n}-\widetilde{s}_N) \cong N\,(\partial\widetilde{s}_N/\partial l_N)\,(l_{N-n}-l_N)$, where

$$\begin{aligned} l_{N-n}-l_N &= \frac{L-R}{N-n}-\frac{L}{N} \\ &= \frac{R-l_Nn}{N}\,[1+O(n/L)]. \end{aligned} \tag{31}$$

The l_N derivative obtains regarding (5) and (9):

$$\frac{\partial\widetilde{s}_N}{\partial l_N} = \frac{1}{a_N}\frac{\partial a_N}{\partial l_N} + a_N = a_N\frac{\partial\sigma_N}{\partial l_N}. \tag{32}$$

Then one expands $\widetilde{s}_{N-n}$ about $\widetilde{s}_N$ regarding (31):

$$\begin{aligned} n\widetilde{s}_{N-n} &\cong n\widetilde{s}_N + n\frac{\partial\widetilde{s}_N}{\partial l_N}(l_{N-n}-l_N) \\ &= n\widetilde{s}_N + O(n/N), \end{aligned} \tag{33}$$

to finally obtain

$$N(\widetilde{s}_{N-n}-\widetilde{s}_N) \cong -a_N\frac{\partial\sigma_N}{\partial l_N}(R-nl_N). \tag{34}$$

Next we show that the $N-n$ th power of the ratio in (30) gives rise to an exponential:

$$\begin{aligned}
&\left[\frac{L-R-(N-n)\sigma_{N-n}}{L-N\sigma_N}\right]^{N-n} \\
=&\ \left(\frac{l_N-\sigma_{N-n}}{l_N-\sigma_N}\right)^{N-n}\left(1-\frac{R-n\sigma_{N-n}}{L-N\sigma_{N-n}}\right)^{N-n} \\
\cong&\ \left(\frac{l_N-\sigma_{N-n}}{l_N-\sigma_N}\right)^{N-n}\exp\left(-\frac{R-n\sigma_N}{l_N-\sigma_N}\right).
\end{aligned} \tag{35}$$

In turn, the first factor in the last line can also be reduced to an exponential whose exponent cancels out the one in Eq. (34) :

$$\begin{aligned}
\left(\frac{l_N-\sigma_{N-n}}{l_N-\sigma_N}\right)^{N-n} &= \left(1+\frac{\sigma_N-\sigma_{N-n}}{l_N-\sigma_N}\right)^{N-n}\cong \\
\left[1+\frac{a_N}{N}\frac{\partial\sigma_N}{\partial l_N}\right]^{N-n} &\cong \exp\left[a_N\frac{\partial\sigma_N}{\partial l_N}(R-nl_N)\right].
\end{aligned} \tag{36}$$

Making use of the results (34)-(36) in formula (30), after some straightforward algebra and convenient rescaling, we obtain the PDF in the final form:

$$g(R)=\frac{1}{\rho}\sum_{n=1}^{n_{\max}}\frac{|R-n\sigma_n|^{n-1}\exp\left\{-\frac{R-n\sigma_N}{l_N-\sigma_N}+n\left[a_n\sigma_n-a_N\sigma_N+\ln\frac{I(a_n)}{I(a_N)}\right]\right\}}{(n-1)!(l_N-\sigma_N)^n}J_n(R)\,. \tag{37}$$

Here $J_n(R)$ is the following integral:

$$\begin{aligned}
J_n(R) &= n\int_{\sigma_m}^{l_m}dl e^{na_n(l-\sigma_n)}\left(\frac{R/n-l}{|R/n-\sigma_n|}\right)^{n-1} \\
&\times\int_{-\infty}^{\infty}\frac{dt}{2\pi}\left[\frac{I_c(t)^2+I_s(t)^2}{I(a_n)^2}\right]^{n/2}\cos[n(lt+\varphi)]\,,
\end{aligned} \tag{38}$$

where $I_c(t), I_s(t), \varphi(t)$ and a_n, σ_n are given in Eqs. (16), (17) and Eqs. (14), (21), respectively. Deriving Eqs. (37) and (38), we changed from the variable L' to $l = L'/n$ so that the upper l integration limit is now $l_m = \min(1, R/n)$. To avoid dealing with extremely small quantities and extremely fast oscillations, we made the following convenient rescaling: we divided $R/n-l$ by $|R/n-\sigma_n|$ and, to compensate, introduced the factor $|R-n\sigma_n|^{n-1}$; similarly, the factor $\exp[na_n\sigma_n + n\ln I(a_n)]$ compensates for the denominator $I(a_n)^n$ and $\exp[-na_n\sigma_n]$ in the integrand.

The maximum $n_{\max}$ in summation of Eq. (37) is the maximum number of disks at close contact which can be put in the space between the particle fixed at $x=0$ and the point $x=R$:

$$n_{\max}(R)=\frac{R-\mathrm{mod}(R,\sigma_m)}{\sigma_m}\,. \tag{39}$$

Note that the expression for $g(R)$ appears to be considerably simpler if no contour shift and rescaling have been applied:

$$\begin{aligned}
g(R) &= \frac{1}{\rho}\sum_{n=1}^{n_{\max}}\frac{n\exp\left(-\frac{R-n\sigma_N}{l_N-\sigma_N}\right)}{(n-1)!(l_N-\sigma_N)^n} \\
&\times\int_{\sigma_m}^{l_m}dl\,(R/n-l)^{n-1}\int_{-\infty}^{\infty}\frac{d\alpha}{2\pi}|I(i\alpha)|^{n/2}\cos[n(l\alpha+\varphi_\alpha)]\,,
\end{aligned} \tag{40}$$

where $I(i\alpha)$ and φ_α are defined in (13). But the formulae (37) and (38) actually provide a much better convergence and much simpler numericals.

3.1.3. The 1D limit

It is important to see how the results obtained for a q1D HD system behave approaching a 1D HD system, i.e., in the limit $D \to 0$ when $\Delta \to 0$, and $\sigma_m, \sigma_n, \sigma_N \to 1$. To this end, we first estimate the x integrals in this limit:

$$\begin{aligned} I(a) &= e^{-a}\Delta + O(\Delta^2), \\ I_c &= e^{-a}\Delta\cos t + O(\Delta^2), \\ I_s &= e^{-a}\Delta\sin t + O(\Delta^2). \end{aligned} \tag{41}$$

As a result,

$$\begin{aligned} \varphi &\to -t, \\ \frac{I_c^2 + I_s^2}{I(a_n)^2} &\to 1, \\ \int_{-\infty}^{\infty} \frac{dt}{2\pi} \left[\frac{I_c^2 + I_s^2}{I(a_n)^2}\right]^{n/2} \cos[n(lt + \varphi)] &\to \delta(l-1), \\ J_n &\to 1. \end{aligned} \tag{42}$$

We see that in the 1D limit, the $g(R)$, Eq. (37), goes over into the Tonks $g_{1D}(R)$, Eq. (27).

3.1.4. Probability to find next neighbor at a distance R

The term with $n = 1$ in the PDF $g(R)$ is proportional to the probability $g_1(R) = Z_{1,R}Z_{N-1,L-R}/\rho Z_{N,L}$ to have next neighbour disk 1 of disk 0 at a distance R including $R < 1$. Here we derive this quantity for an infinitely long q1D HD system. The case $n = 1$ is particular because the small distance between neighbor disks sets certain restriction on the integration over their transverse coordinates y which depends on their distributions. Now we have to consider the two neighbor disks, 0 and 1, within the large system. The result is similar to that obtained in [19] in deriving the y distribution across the pore. This distribution has the form $\propto \varphi(y)^2$ where φ is the following integral:

$$\varphi(y) = \int_{-\Delta/2}^{\Delta/2} dy' e^{-\alpha_N \sigma(y-y')}. \tag{43}$$

Here $\sigma(y - y')$ is defined in eq.(1), and, compared with formulae of [19], the integration variable σ is changed to y. This derivation shows that to place the two disks into a large system, it is sufficient to consider correlations between disk 0 and one disk on the left of disk 0, call it disk -1, and that between disk 1 and one disk, call it disk 2, on the right of disk 1. Then, rather than disks 0 and 1 we consider disks $-1, 0, 1$, and 2 which results in the following extensions:

$$\int_{-\Delta/2}^{\Delta/2} dy_0 \;\to\; \int_{-\Delta/2}^{\Delta/2} dy_{-1} \int_{-\Delta/2}^{\Delta/2} dy_0 e^{-\alpha_N \sigma(y_0 - y_{-1})} = \int_{-\Delta/2}^{\Delta/2} dy_0 \varphi(y_0),$$

$$\int_{-\Delta/2}^{\Delta/2} dy_1 \;\to\; \int_{-\Delta/2}^{\Delta/2} dy_1 \int_{-\Delta/2}^{\Delta/2} dy_2 e^{-\alpha_N \sigma(y_2 - y_1)} = \int_{-\Delta/2}^{\Delta/2} dy_1 \varphi(y_1).$$

Regarding the equalities $\sigma_{N-1} = \sigma_{N+1}$ and $\widetilde{s}_{N-1} = \widetilde{s}_{N+1}$ valid up to $O(1/N)$ and retaining only the R dependent terms $z(R)$, one has:

$$z(R) = \int_{-\Delta/2}^{\Delta/2} dy_0 \int_{-\Delta/2}^{\Delta/2} dy_1 \varphi(y_0)\varphi(y_1)\theta\left[R^2 + (y_0 - y_1)^2 - 1\right] \exp(-a_N R), \tag{44}$$

where the θ function eliminates states in which the cores of disks 0 and 1 overlap and we used that $1/(l_N - \sigma_N) = a_N$. Normalizing on unity, one finally obtains:

$$g_1(R) = \frac{z(R)}{\displaystyle\int_{\sigma_m}^{\infty} dRz(R)} . \tag{45}$$

In relation with the approximation used to derive the PF (3) and described in Sec.2, we stress that the distribution $\varphi(y)^2$ with φ given in (43) is very different from that in the system periodic in the y direction [4], and the approximation influences this distribution only through the value of a_N.

4. Results and discussion

Figures 2 and 3 present the PDF $g_1(R)$ for next neighbor disks obtained from Eq. (45) for a set of linear densities $\rho = N/L$ and two reduced pore widths Δ. The sharp peak at $R = 1$ is present at all densities including very high, but in this case its height is incomparable with second peak centered at the average interdisk spacing $l_N = 1/\rho$. The second peak appears and strengthens as density becomes higher and higher. The concentration of spacings R at the average distance indicates a high order along the pore. For densities ρ near the close packing, this also implies a high overall zigzag order since $R \cong l_N$ approaches the minimum separation σ_m for which disks stay very close to the walls. In contrast, the fact that there is a high peak at $R = 1$ which is particularly pronounced for the density $\rho = 1$ with $l_N = 1$ shows that the ordering at this density is not necessarily related with a zigzag type order. We shall give this issue a more consideration later on as the peculiarity of separation $R = 1$ and density $\rho = 1$ will get additional indications. Right now we would like only to explain the very reason for the cusp at $R = 1$ whose presence at PDFs $g_1(R)$ and $g(x)$ has been well known [7, 8, 19, 24, 11]. To this end, the θ function in the formula for $z(R)$, Eq. (44), is replaced by the explicit dependence of the integration limits on R, i.e.,

$$z(R) = \begin{cases} \displaystyle\int_{-\Delta/2}^{\Delta/2-\sqrt{1-R^2}} dy_0 \int_{y_0+\sqrt{1-R^2}}^{\Delta/2} dy_1 \varphi(y_0)\varphi(y_1), \quad R \leq 1 , \\ \displaystyle\int_{-\Delta/2}^{\Delta/2} dy_0 \int_{-\Delta/2}^{\Delta/2} dy_1 \varphi(y_0)\varphi(y_1), \quad R > 1 . \end{cases} \tag{46}$$

This formula shows that the increase of the disk transverse free path in y with distance R abruptly stops at its maximum constant value Δ at $R = 1$.

In Fig. 2a, the theoretical $g_1(R)$ is superimposed on the MD simulation data [24] for the same $\Delta = 0.5$. It is seen that the theoretical and MD simulation results for high $\rho = 1.111$ and low $\rho = 0.8$ practically coincide whereas for the intermediate densities $\rho = 1.053$ and 1.01 they look very different. Actually, however, a perfect fit can be achieved by a small increase of these theoretical densities respectively to 1.065 and 1.032, Fig. 2b. This mismatch is addressed after presenting the case of pore width $\Delta = 0.866$ in Fig. 3. This figure shows our theoretical $g_1(R)$ for the densities for which in [7] the PDF normalized on the density, g/ρ, was obtained by a Monte Carlo simulation for short distances $R < 1.5$. While $g_1(R)$ contains the contribution of a single next neighbor, $g(R)$ in [7] includes the contributions of both next and next-next neighbor. Nevertheless, the peaks for $\rho = 1.6$ and 1.4 are concentrated at distances $R < 1$ where the contribution of the next-next neighbor is indirect and negligible so that our g_1/ρ and the g/ρ can be compared. After dividing by the correspondent ρ, these curves in Fig.3 become in a good agreement with their counterparts from [7]. The results for $\rho = 1$ and 0.6, however, cannot be compared as the role of the next-next neighbor for these curves in [7] is essential.

The first idea is that the reason for the aforementioned mismatch lies in the approximation described in Sec.2 which was used in the derivation of the PF in [19]. This can be checked by developing the theory which does not use both above approximation and periodic boundary condition in the x direction. At the same time, to address the mismatch between our theoretical and MD results at the intermediate densities for $\Delta = 0.5$, it is also important to resort to Fig. 4 which presents our theoretical $g(R)$ and the MD results for $\rho = 1$. Figure 4a shows that the general trend is that the theoretical peaks obtained for an infinitely long system are slightly wider and lower than those obtained by the MD simulations for a system with periodic boundary conditions. The theoretical correlation length $1/0.124 \approx 8.1$ is

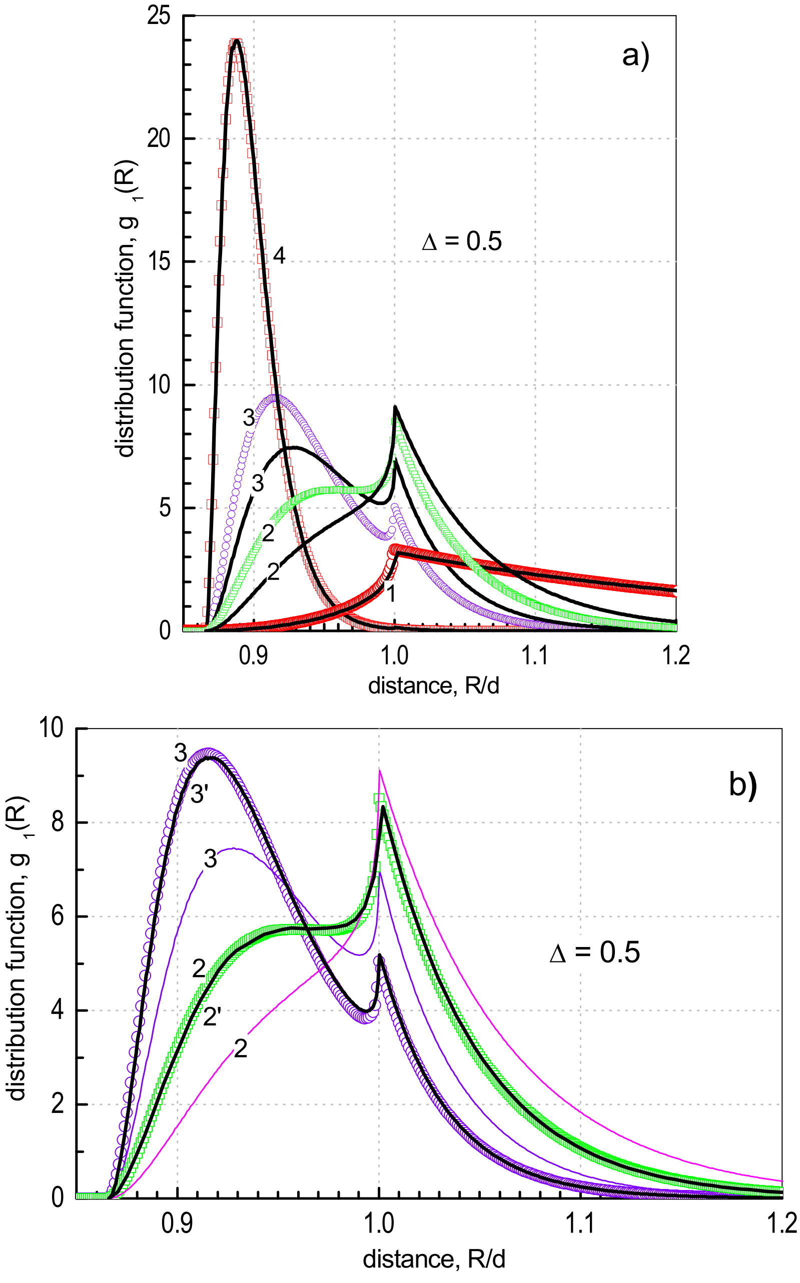

Figure 2. Part a): Theoretical results (solid lines) and MD simulation data (symbols) for pair distribution function $g_1(R)$ for pore width $\Delta = 0.5$ and four densities: $1 - \rho = 0.8$; $2 - 1.01$; $3 - 1.053$; $4 - 1.111$. Part b): Theoretical results for shifted densities $\rho = 1.034$ and $\rho = 1.065$ (thick solid lines) which are practically indistinguishable of the MD simulation data (symbols) for densities $\rho = 1.01$ (right peak) and $\rho = 1.053$ (leftt peak), respectively. For comparison, the thin solid lines 2 and 3 [the same as in part a)] show theoretical curves for actual (non shifted) densities $\rho = 1.01$ and 1.053, respectively .

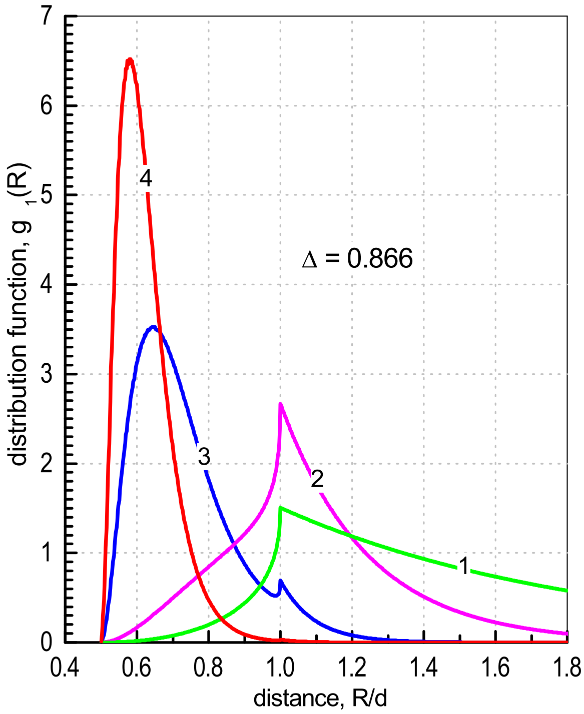

Figure 3. Theoretical pair distribution function $g_1(R)$ for pore width $\Delta = 0.866$ and four different densities: 1 – $\rho = 0.6$; 2 – 1; 3 – 1.4 and 4 – 1.6.

slightly shorter than that of the fit to MD data $1/0.1015 \approx 9.85$, Fig. 4b. This last figure, however, also demonstrates a visually appreciable difference between the theoretical and MD $g(R)$: the last does not vanish for large R and remains at a level on the order of 0.01 for both system sizes $N = 400$ and $N = 2000$. The residual correlations persist for all $R \gtrsim 50$, are highly fluctuating, showing no tendency to decreasing and are even higher for the larger system. This points to the possibility that the slower correlation decay of MD data is connected to the system finite size, i.e., the effect which was already addressed in [11]. Another reason can be the periodic boundary conditions employed in MD simulations: imposing a correlation at the distance equal to the system length L can also enforce the longitudinal correlation value. The relation between theoretical and computer simulation data was already addressed in [16] where we compared the data for the transverse disk distributions. It was found that the former always predict less disks at the walls, i.e., at $R \sim \sigma_m$, and slightly more disks at a distance $R \sim 1$ than the latter. The reason is that the space for windowlike defects with $R \sim 1$ is related to the system size L: it diminishes sharper with the linear density ρ for shorter L and for sufficiently high ρ in a finite size system is not available at all. At the same time, the probability of a window $R \sim 1$ in the zigzag arrangement in an infinite q1D system is nonzero for any ρ below close packing [19]. For this reason it can be expected that the peaks of $g_1(R)$ and $g(R)$ in an infinite theoretical system are slightly stretched toward higher R, hence are wider and slightly lower than those obtained in computer simulations of a finite system with periodic boundary conditions, which is the case of Fig.4. In terms of correlation decay, this means that an infinite system has a shorter correlation length than that in a finite system with periodic boundary conditions. Clearly, in terms of pressure and density it implies that the pressure sensitively depends on the ordering details: in a finite system pressure is slightly higher than in an infinite system and the mismatch between the two PDFs can be eliminated by shifting the density of an infinite system to a slightly higher value, which was demonstrated in Fig.2b. Another question is why this shift is mostly needed at the intermediate densities, i.e., those between the dense packing and gas values. Before addressing this we first consider the results presented in Figs. 5 and 6.

The longitudinal pair correlations as function of the disks' number difference, $g_2(|n_2-n_1|)$, has been investigated in detail by the transfer matrix method [6, 8, 9, 10, 11]. At the same time, the PDF $g(R)$ as function of the disk separation R for given density cannot be directly obtained by this method. Formula (37) considerably simplifies its calculation

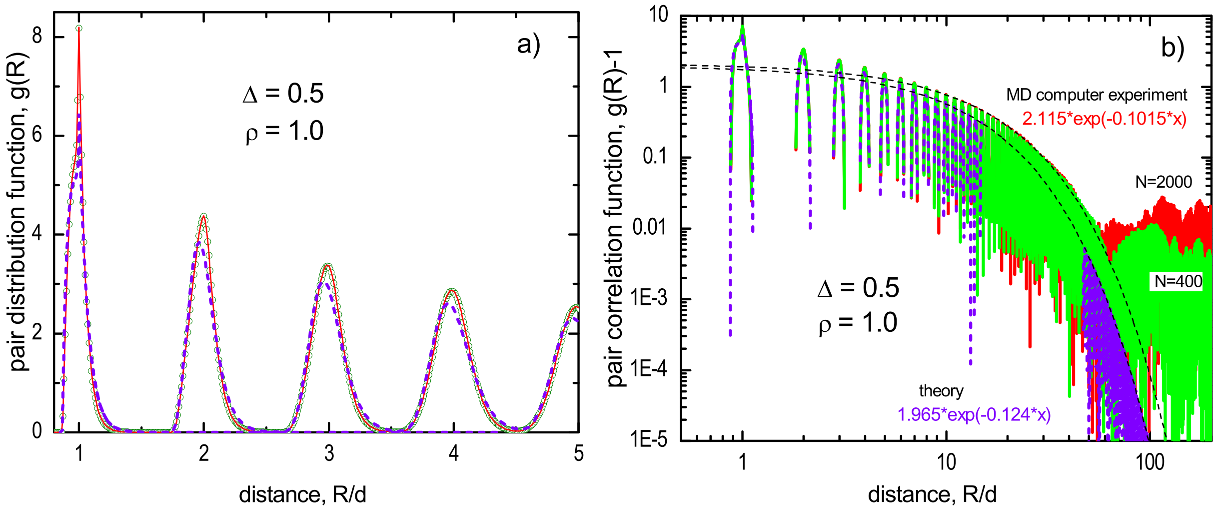

Figure 4. Theoretical PDF $g(R)$ (the dashed line) superimposed on MD simulation data (the solid line and symbols) for the case of pore width $\Delta = 0.5$ and density $\rho = 1$. The MD data are shown for two distinct sizes of the simulated system, i.e., $N = 400$ (the green color) and $N = 2000$ (the red color). Part a) for distances $R < 5$ and part b) for distances $R < 200$. In part b) the theoretical curve is cropped in the range $15 < R/d < 50$ for better visualization of the simulation data.

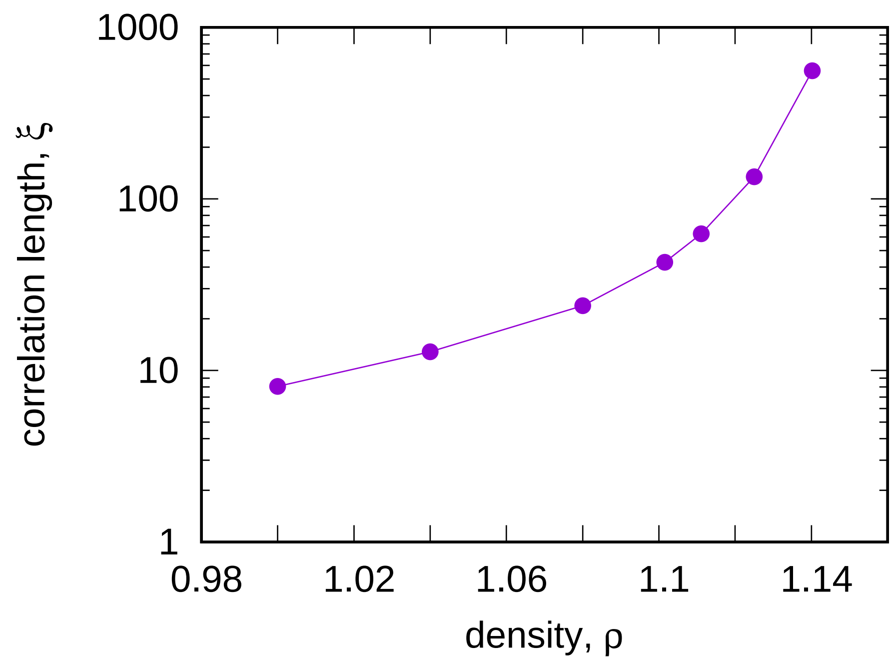

Figure 5. Dependence of the correlation length ξ on density ρ for the case of pore width $\Delta = 0.5$.

and enables one to get its systematic understanding by means of the direct calculation. The density ρ determines a_N (i.e., the pressure) via simple transcendental Eq. (5) in which Δ enters via minimum contact distance σ_m, Eq. (1), and σ_N is given by Eq. (9). We obtained the PDF $g(R)$, Eq. (37), by performing the integration in Eq. (38) numerically, Figs. 5 and 6 [25]. Contrary to our suggestion based on computer simulations data [24] and in line with the results of the transfer matrix method [11], our findings on the longitudinal correlations in the thermodynamic limit show an exponential decay for all pore widths and densities. The correlation length is a monotonically increasing function of density, Fig. 5. To combine both width and density effects, we fixed the ratio $(\rho/\rho_{\max})$ of the actual density ρ to the maximum density $\rho_{\max}(\Delta)$ for a given pore width Δ, and then found the correlation lengths for different Δ in the total range of the single-file widths, $0 \leq \Delta \leq \sqrt{3}/2 \approx 0.866$, Fig. 6. For a given Δ the maximum density is $\rho_{\max}(\Delta) = 1/\sigma_m(\Delta) = 1/\sqrt{1-\Delta^2}$. It follows that as Δ runs from 0 to 0.866, the actual density $\rho = (\rho/\rho_{\max})/\sqrt{1-\Delta^2}$ monotonically increases from 0 to $1.1547(\rho/\rho_{\max})$. In particular, for the same Δ, the actual ρ is higher for higher $\rho/\rho_{\max}$. The results for $(\rho/\rho_{\max}) = 0.866$, 0.9539 and 0.9875 are presented in Fig. 6.

First, it is seen that, for the same Δ, the correlation length is larger for a higher density. Second, as the width approaches zero, the correlation length tends to the value obtained for the 1D Tonks gas from $g_{1D}(R)$, Eq. (25). Third, the width and density monotonically grow along the curves in Fig.$\tilde{6}$. It is seen however that the correlation length does not monotonically increase as both the width and density do: there is a maximum at each of the three curves. But the most interesting observation is that all these maxima occur at the density $\rho = 1$ when a pore length interval equal to the disk diameter d is on average occupied by one disk. This is another peculiarity of these density and disks' separation indicated above.

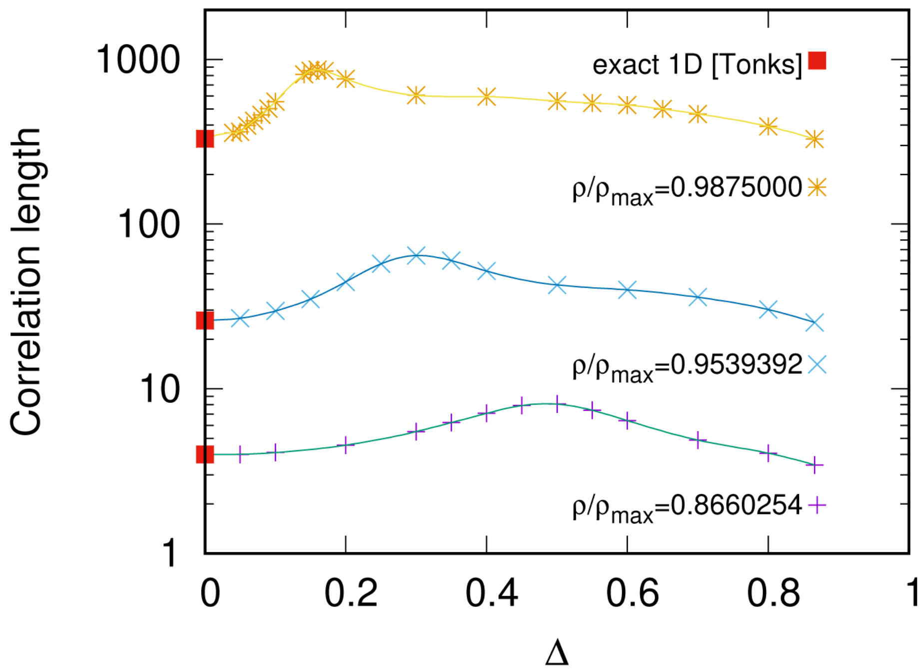

Figure 6. Numerically obtained correlation length (symbols) for the correlation function $g(R) - 1$ as a function of width Δ for the fixed ratio $(\rho/\rho_{\max})$ [for given pore width Δ, the maximum density $\rho_{\max} = 1/\sigma_m(\Delta)$]. The three curves correspond to the three different ratios $(\rho/\rho_{\max})$ indicated in the figure. All maxima on different curves appear at density $\rho = 1$.

Thus, Figs. 2, 3, and 6 show that the PDFs $g_1(R)$ and $g(R)$ have peculiarities at the density $\rho = 1$ in the form of certain peaks or maxima. Moreover, for $\Delta = 0.5$, density $\rho = 1$ is in the intermediate range between high and low densities where we found a high sensitivity of the pressure to density. Consider this effect which can be related to the mismatch between the correlations in an infinite and finite system with periodic boundary condition. It has been suggested that the peak at the distribution of next neighbors at $R = 1$, Figs.2, 3, is related to the tendency of the system to produce windowlike defects to increase the entropy as such a defect enables disk's travel across the pore

[27, 9, 19, 24]. However, our finding that the correlation length has a maximum at $\rho = 1$ for any pore width, Fig.6, is unexpected and cannot be explained by this idea alone. At higher densities, the peak at $R = 1$ is diminishing and the peak at another distinguished, namely average distance $l_N = L/N < 1$ is raising and eventually dominates the one at $R = 1$. As the peak of $g_1(R)$ at $R = L/N$ is definitely related to the longitudinal component of the zigzag order, it is natural to connect the peak at $\rho = 1$, at least partially, to the nascent longitudinal ordering, too. In the light of this idea, the maxima of the correlation length become reminiscent of the correlation length increase at a phase transition. Of course, there is no transition at $\rho = 1$, but a kind of pretransitional effect seems to show up. Interestingly, in recent paper on the same q1D HD system [28], the authors found, also for all widths Δ's, well developed compressibility peaks at $\rho \approx 1$ showing that at this density the system is softer even than at lower densities, which is in line with the above idea. We may then speculate that at $\rho = 1$, this effect is somehow related to the increase of the correlation length and to enforced correlation sensitivity at densities in the vicinity of $\rho = 1$. Approaching thermodynamic equilibrium, a system tends to find more space to increase its entropy. For densities near close packing, it has no much choice: the interdisk space is very limited, correlating many such spacings along the system requires extremely fine adjustments so that the correlations are determined by the average distance L/N. At low densities, the interdisk spacings are large and uncorrelated, so that again entropy-wise the correlations are connected to L/N rather than to the global system's size. But at the intermediate densities, when the longitudinal and nascent transverse orders compete, the system tends to benefit from both interdisk spaces, the strict L/N and those nearby $L/N \sim 1$. To do so, it searches for the space by correlating interdisk spaces along the system so that the system size comes into play. As a result, the size effect can manifest itself in the pressure: slight increase of density adjusts the pressure in an infinite system to that in a finite one.

5. Conclusion

We derived the formulae for the two important PDFs $g(R)$ and $g_1(R)$ for a q1D HD system and demonstrated that they can be readily used. Apart of that, based on our finding on the correlation lengths, we suggested that the density $\rho = 1$ plays a distinguished role in the zigzag transformation with density irrespective of the pore width. We related this to a nascent longitudinal order and the system tendency to correlate multiple interdisk spacings along the system to increase its entropy. To this effect we attributed the high sensitivity of the system pressure to its density in the vicinity of $\rho = 1$ which was also revealed in [28]. As the pressure is affected by a system size and can be slightly higher in a finite system with periodic boundary conditions than in an infinite system, the PDF $g(R)$ and next-neighbor distribution $g_1(R)$, which nearly coincide with computer simulation data for high and low densities, can differ for intermediate densities in the vicinity of $\rho = 1$, but can be made coinciding by the correspondent density increase in an infinite system. Of course, one obvious reason for the observed mismatch between the theoretical predictions and simulation data can be the approximation described in Sec.2, but one cannot also exclude an effect of the pressure difference between a finite system with the periodic boundary condition and infinite system, which is possible at the intermediate densities. Note that the theoretical results [11, 26] based on the transfer martrix approach show a good fit to the simulation data for high, low, and intermediate densities. As the periodic boundary conditions along the pore are essential for both these approaches, the relation between the results obtained for a finite and infinite systems is yet to be clarified. The investigation of a similar problem in the physics of one-dimensional ultra cold quantum gases shows that this problem is nontrivial and worth to be addressed [29].

Declaration of competing interest

The authors declare that they have no known competing financial interests or personal relationships that could have appeared to influence the work reported in this paper.

Acknowledgments

V.M.P. is grateful to Center for Theoretical Physics PAS for hospitality. V.M.P.'s research is part of the project No. 2022/45/P/ST3/04237 co-funded by the National Science Centre and the European Union Framework Programme for Research and Innovation Horizon 2020 under the Marie Skłodowska-Curie grant agreement No. 945339. T.B. and A.T. were supported by the National Research Foundation of Ukraine under the grant 2020.02/0115.

References

[1] E. H. Lieb, D. C. Mattis, Mathematical Physics in One Dimension: Exactly Soluble Models of Interacting Particles, Academic, New York, 2013.

[2] L. Tonks, The complete equation of state of one, two and three-dimensional gases of hard elastic spheres, Phys. Rev. 50 (1936) 955-963. https://doi.org/10.1103/PhysRev.50.955

[3] K.W. Wojciechowski, P. Pieranski, J. Małecki, A hard-disk system in a narrow box. I. Thermodynamic properties, J. Chem. Phys. 76, 6170-6175 (1982). https://doi.org/10.1063/1.443019

[4] D.A. Kofke, A.J. Post, Hard particles in narrow pores. Transfer-matrix solution and the periodic narrow box, J. Chem. Phys. 98 (1993) 4853-4861. https://doi.org/10.1063/1.479206

[5] H. A. Kramers, G. H. Wannier, Statistics of the Two-Dimensional Ferromagnet. Part I, Phys. Rev. 60 (1941) 252-262. https://doi.org/10.1103/PhysRev.60.252.

[6] S. Varga, G. Balló, P. Gurin, Structural properties of hard disks in a narrow tube, J. Stat. Mech. Theory Exp. P11006 (2011). 10.1088/1742-5468/2011/11/P11006

[7] P. Gurin, S. Varga, Pair correlation functions of two- and three-dimensional hard-core fluidsconfined into narrow pores: Exact results from transfer-matrix method, J. Chem. Phys. 139 (2013) 244708-6.

[8] M. Godfrey, M. Moore, Understanding the ideal glass transition: Lessons from an equilibrium study of hard disks in a channel, Phys. Rev. E 91 (2015) 022120-15. https://doi.org/10.1103/PhysRevE.91.022120

[9] J.F. Robinson, M.J. Godfrey, M.A. Moore, Glasslike behavior of a hard-disk fluid confined to a narrow channel, Phys. Rev. E 93 (2016) 032101-10. https://doi.org/10.1103/PhysRevE.93.032101

[10] Y. Hu, L. Fu, P. Charbonneau, Correlation lengths in quas-ione-dimensional systems via transfer matrices, Mol. Phys. 116 (2018) 3345-3354. https://doi.org/10.1080/00268976.2018.1479543

[11] Y. Hu, P. Charbonneau, Comment on “Kosterlitz-Thouless-type caging-uncaging transition in a quasi-one-dimensional hard disk system”, Phys. Rev. Research 3 (2021) 038001-5. https://doi.org/10.1103/PhysRevResearch.3.038001

[12] P. Gurin, G. Odriozola, S. Varga, Critical behavior of hard squares in strong confinement, Phys. Rev. E 95 (2017) 042610-10. https://doi.org/10.1103/PhysRevE.95.042610.S.

[13] K.K. Mon, Virial series expansion and Monte Carlo studies of equation of state for hard spheres in narrow cylindrical pores, Phys. Rev. E 97 (2018) 052114-7. https://doi.org/10.1103/PhysRevE.97.052114

[14] M.Z. Yamchi, S.S. Ashwin, R.K. Bowles, Inherent structures, fragility, and jamming: Insights from quasi-one-dimensional hard disks, Phys. Rev. E 91 (2015) 022301-12. https://doi.org/10.1103/PhysRevE.91.022301

[15] C.L. Hicks, M.J. Wheatley, M.J. Godfrey, M.A. Moor, Gardner Transition in Physical Dimensions,

[16] A. Huerta, T. Bryk, V.M. Pergamenshchik, A. Trokhymchuk, Collective dynamics in quasi-one-dimensional hard disk system, Frontiers in Physics 9 (2021) 636052-15. https://doi.org/10.1103/PhysRevLett.120.225501

[17] M.F. Holovko, V.I. Shmotolokha, W. Dong, Analytical theory of one- and two-dimensional hard sphere fluids in random porous media, Cond. Matter Phys. 13 (2010) 23607-7. http://dspace.nbuv.gov.ua/handle/123456789/32097

[18] M.A. Cazalilla, R. Citro, T. Giamarchi, E. Orignac, M. Rigol, One dimensional bosons: From condensed matter systems to ultracold gases, Rev. Mod. Phys. 83 (2011) 1405-1466. https://doi.org/10.1103/RevModPhys.83.1405

[19] V.M. Pergamenshchik, Analytical canonical partition function of a quasi-one-dimensional system of hard disks. J. Chem. Phys. 153 (2020) 144111-10. https://doi.org/10.1063/5.0025645

[20] I.R. Yukhnovski, M.F. Holovko, Statistical Theory of Classical Equilibrium Systems, Naukova Dumka, Kyiv, 1980 (in Russian).

[21] A. Santos, A Concise Course on the Theory of Classical Liquids. Basics and Selected Topics, Lecture Notes in Physics, Vol. 923, Springer International Publishing, Switzerland, 2016. https://doi.org/10.1007/978-3-319-29668-5

[22] J. Frenkel, Kinetic Theory of Liquids, Dover Publications, NY, 1946.

[23] T. Nagamiya. Statistical mechanics of one-dimensional subtances I, Proc. Phys.-Math. Soc. Japan 22 (1940) 705-729. https://doi.org/10.11429/ppmsj1919.22.8-9_705

[24] A. Huerta, T.M. Bryk, V.M. Pergamenshchik, A.D. Trokhymchuk, Kosterlitz-Thouless-type caging-uncaging transition in a quasi-one-dimensional hard disk system, Phys. Rev. Research 2 (2020) 033351-5. https://doi.org/10.1103/PhysRevResearch.2.033351

[25] After this paper was submitted, Montero and Santos presented their analytical theory of $g(R)$ which is based on the formulae equivalent to the transfer matrix approach with the periodic boundary condition [26].

[26] A.M. Montero, A. Santos, Structural properties of hard-disk fluids under single-file confinement, arXiiv: 2304.14290v1 (2023). https://arxiv.org/abs/2304.14290

[27] R.K. Bowles, I. Saika-Voivod, Landscapes, dynamic heterogeneity, and kinetic facilitation in a simple off-lattice model, Phys. Rev. E 73 (2006) 011503-4 . https://doi.org/10.1103/PhysRevE.73.011503

[28] A.M. Montero, A. Santos, Equation of state of hard-disk fluids under single-file confinement, J. Chem. Phys. 158 (2023) 154501-5. doi:10.1063/5.0139116

[29] M.T. Batchelor, X.W. Guan, N. Oelkers, C. Lee, The 1D interacting Bose gas in a hard wall box, J. Phys. A 38 (2005) 7787. DOI 10.1088/0305-4470/38/36/001